

**Resonant Raman scattering from polyacetylene and poly(*p*-phenylene vinylene)  
chains included into hydrogenated amorphous carbon**

M. Rybachuk<sup>1,3\*</sup>, A. Hu<sup>2</sup>, J.M. Bell<sup>3</sup>

<sup>1</sup> *Federal Institute for Materials Research and Testing (BAM), Division VI.4 Surface  
Technology, Unter den Eichen 87, 12205 Berlin, Germany*

<sup>2</sup> *Department of Physics, University of Waterloo, 200 Univ. Ave. West, Waterloo, ON,  
N2L 3G1, Canada*

<sup>3</sup> *Faculty of Built Environment and Engineering, Queensland University of  
Technology, 2 George St, Brisbane, Qld 4001, Australia*

**ABSTRACT**

The resonant Raman scattering in N-IR – UV range from amorphous hydrogenated carbon (*a*-C:H) reveal inclusions of trans-polyacetylene (*trans*-(CH)<sub>x</sub>) chains with approximate length of up to 120 C=C units and inclusions of poly(*p*-phenylene vinylene) (PPV) polymer chains. The PPV is evidenced by a strong dispersive mode at *ca.* 1175 cm<sup>-1</sup>. It was found that the Raman response from core *A<sub>g</sub>* *trans*-(CH)<sub>x</sub> modes incorporated into *a*-C:H to changing excitation energy is identical to of free-standing chains thus facilitating identification of *trans*-(CH)<sub>x</sub> in complex carbonaceous materials spectra.

PACS number(s): 81.05.Uw, 73.50.-h, 71.23.-k, 78.30.-j, 61.41.+e.

## MAIN TEXT

It is known that diamond-like carbon (DLC) can host a basic polymer, the *trans* isomer of polyacetylene (*trans*-(CH)<sub>x</sub>) initially reported for CVD grown diamond<sup>1</sup> and later found in low temperature grown hydrogenated amorphous carbon (*a*-C:H) films<sup>2</sup>. Excellent conductivity of *trans*-(CH)<sub>x</sub> due to strong electron-phonon (*e*-ph) and electron-electron coupling originating from delocalised  $\pi$  electrons and an effective lattice nonlinearity<sup>3,4</sup> and the large third-order nonlinear optical susceptibility that allows the chain to withstand high peak pump powers without damage to the sample, ensure considerable interest in this polymer as a non-linear optical material<sup>5</sup>. Achieving controlled inclusion of *trans*-(CH)<sub>x</sub> into host DLC has been difficult and only short ( $\leq 20$  of *C=C* units) *trans*-(CH)<sub>x</sub> segments have been found to date<sup>1,6</sup>. Recently, Hu *et al.*<sup>7,8</sup> demonstrated that variably bonded carbon atoms, including *trans*-(CH)<sub>x</sub>, can be incorporated on a carbon surface using ultra-short laser pulses. Apart from *trans*-(CH)<sub>x</sub> segments DLC can also contain nanoparticles like carbon onions<sup>9</sup> or spherical nanocrystallites as reported by Chen *et al.*<sup>10</sup>. These greatly reduce internal stress and thus are favourable for tribological applications.

We present here a resonant Raman scattering (RRS) investigation of *a*-C:H films synthesised in a low temperature inductively coupled plasma (ICP) reactor<sup>11</sup>. Although films are indeed of low stress and host *trans*-(CH)<sub>x</sub> chains of significant length ( $\leq 120$  of *C=C* units), they also contain poly(*p*-phenylene vinylene) (PPV)

inclusions that have not been reported previously. The RRS technique probes atomic configurations in materials via the vibrational density of states<sup>3,6,12</sup> and in this work laser excitation energies,  $\hbar\omega_L$  ranging from 1.58 eV (N-IR) to 5.08 eV (UV) are used, ensuring bonding and structural disorder in the great majority of  $sp^3$ ,  $sp^2$  and  $sp$  carbon mixtures are studied. We also demonstrate that the response of  $trans-(CH)_x$  segments in  $a-C:H$  to changing excitation energy is identical to that of free-standing isolated  $trans-(CH)_x$  chains, both empirically and theoretically, using either the bimodal distribution model proposed by Brivio *et al.*<sup>13</sup> or the amplitude mode theory proposed by Ehrenfreund *et al.*<sup>3</sup>. Our findings exemplify an approach which facilitates the extraction of  $trans-(CH)_x$  contributions from the core  $a-C:H$ , DLC or carbonaceous materials spectra thus precluding overfitting as in case of Piazza *et al.*<sup>2</sup>.

$a-C:H$  films were deposited on *Si* at the rate of  $\sim 30$  nm/hour using  $CH_4/Ar$  plasma in Helmholtz type ICP reactor<sup>11</sup> at temperatures of  $\leq 400$  K as described elsewhere<sup>14</sup>. The deposition pressure was  $\sim 6 \times 10^{-2}$  Pa and the substrate was negatively DC biased at 250-300 V. The fabricated films were of low stress  $\leq 1$  GPa, with hardness of  $\leq 20$  GPa and a friction coefficient of 0.07 at 70 % humidity as measured by nano-mechanical testing (UMIS). Electrical resistivity was  $\geq 8 \times 10^8 \Omega$  cm. Films were  $\sim 140$  nm thick with a maximum refractive index of 2.2 in the UV-blue region measured by IR-UV spectroscopic ellipsometry (J.A. Woollam Co.) The hydrogen content was found to be 27.5 ( $\pm 2.5$ ) at. % for all films as determined from Fourier Transform infrared (FT-IR) spectroscopy (Nicolet Nexus). Analysis of  $C_{1s}$  and valence bands of X-ray photoelectron spectra (Kratos Axis Ultra) determined the  $sp$ ,  $sp^2$  and  $sp^3$  contents to be 2, 68 and 30 % respectively with the uncertainty of 1.25 %. The  $sp$ -hybridised content was verified using Raman and FT-IR, and the  $sp^3$  content using 244 nm Raman results<sup>12</sup>. Unpolarised Raman spectra (5.08 - 1.58 eV) were

obtained *ex situ* at 293 K using 244, 532, 633 and 785 nm Renishaw instruments and 325 nm and 442 nm Kimmon Raman instruments. All excitation wavelengths excluding 785 nm were pulsed; the 785 nm was a continuous wavelength laser source. The frequency-doubled *Ar* ion laser was used for 244 nm, *He/Cd* for 325 nm and 442 nm, the frequency-doubled YAG laser was used for 532 nm, *He/Ne* gas laser was used for 633 nm and a diode laser source was used for 785 nm excitations. All measurements were taken in dynamic mode where a specimen is moved linearly at speeds of  $\leq 30 \mu\text{m/s}$  and laser power was kept  $< 1 \text{ mW}$  minimizing thermal damage.

Fig. 1 shows RRS spectra of an *a*-C:H film. After a linear background subtraction the spectra were all fitted with Gaussian line-shapes using a nonlinear least squares fitting<sup>15</sup>. Fitted bands are the common DLC *D* and *G* modes (N-IR and visible) and *T* mode (UV)<sup>12</sup> and the two  $A_g$  zone center vibrational modes of *trans*-(CH)<sub>x</sub><sup>3,4,13</sup>: the C-C  $\omega_1$  at  $\sim 1060 \text{ cm}^{-1}$ , and the C=C backbone stretching  $\omega_3$  mode at  $\sim 1450 \text{ cm}^{-1}$ . The weak  $\omega_2$  mode at  $\sim 1280 \text{ cm}^{-1}$  was not detectable though its contributions may be obscured by the *D* and  $\omega_1$  bands. The absorption for bulk *trans*-(CH)<sub>x</sub> occurs at 1.5 - 1.7 eV<sup>4,13</sup> and corresponds to positions of the  $A_g$  zone centres at 1060, 1280 and 1450  $\text{cm}^{-1}$ . This applies for N-IR excitation. As  $\hbar\omega_L$  increases moving away from resonance, shoulders appear at the high frequency side of the  $\omega_1$  and  $\omega_3$  modes, eventually developing into secondary peaks<sup>3,13,16</sup> at excitation energies well above the band gap of 2.71 eV<sup>4</sup>. The RRS spectra disperse<sup>6</sup> and these peaks change in intensity (*I*) and widths ( *$\Gamma$* ). The complexity of separating intercalated *trans*-(CH)<sub>x</sub> from the host DLC modes lead us to analyse a single symmetric band distribution. This proved to be sufficient<sup>3</sup> to account for a double peak Raman structure.

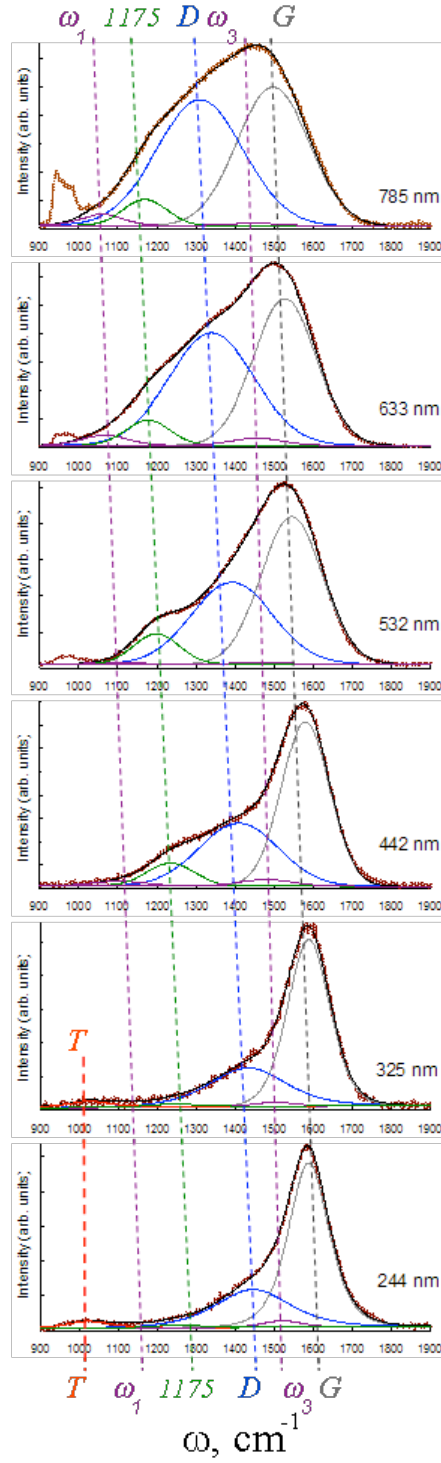


FIG. 1. The RRS spectra of examined  $a$ -C:H films showing contributions from  $trans$ - $(\text{CH})_x$  ( $\omega_1$  and  $\omega_3$  modes), PPV ( $1175 \text{ cm}^{-1}$  mode) and DLC ( $D$ ,  $G$  and  $T$  modes). An asymmetric peak visible at N-IR – visible (green)  $\hbar\omega_L$  at  $\sim 950 \text{ cm}^{-1}$  is the second order  $Si$ .

A peak positioned at  $1175 \text{ cm}^{-1}$  at N-IR  $\hbar\omega_L$  we assign to a  $CC-H$  bending mode of the ring in neutral poly(*p*-phenylene vinylene)<sup>17-19</sup>. The origin of this mode could be due to introduction of heteroatoms (defects) in  $sp^2$  rings since in single crystals these lead to a relaxation of wave vector  $k=0$  selection rule<sup>6,12</sup> thus providing a mechanism for phonons from outside the centre of the Brillouin zone to contribute to the Raman scattering. Introduction of heteroatoms allows delocalisation of  $\pi$  electrons confined to the  $sp^2$  rings and thus dispersion<sup>12,17</sup>.

Other PPV zone centre vibrational modes should be positioned at higher frequencies in the ranges<sup>18,19</sup>  $1200 - 1330$  and  $1540 - 1625 \text{ cm}^{-1}$ , but these are certainly obscured by the host  $D$  and the  $G$  modes. The large width of the  $1175 \text{ cm}^{-1}$  mode suggests a combination of a vinylene and a  $CC-H$  ring bend modes since the zone mode frequency for vinylene<sup>20</sup> is at  $1145 \text{ cm}^{-1}$ .

As  $\hbar\omega_L$  energy increases all peaks shift to a higher frequency; DLC modes are obeying phonon confinement rules<sup>12</sup>, Fig. 2 (a) shows peak dispersion,  $\Delta\omega$ , the shift in peak position relative to the N-IR excitation peak position. Fig. 2 (b) summarizes changes in  $\Gamma$  for all fitted peaks. The steady  $I(D)/I(G)$  ratio decrease from  $\sim 0.9$  to  $0.2$ , pronounced reduction in  $\Gamma_D$  and  $\Gamma_G$  and the  $G$  peak saturation<sup>12</sup> at  $\sim 1590$  for  $244 \text{ nm}$  excitation are indicative of a highly ordered and symmetric  $sp^2$  phase<sup>12,14</sup>. The band gap for PPV is  $2.2 - 2.3 \text{ eV}$ <sup>18</sup> and that is selectively probed by a resonance frequency of green  $532 \text{ nm}$  laser; Fig. 1 shows the elevated intensity,  $I_{1175}$  and Fig. 2 (b) the broadening peak width,  $\Gamma_{1175}$  for the PPV peak. This peak is almost certainly of  $sp^2$  origin since its contributions disappear in UV excitation. There is an increase in  $I(\omega_3)/I(\omega_1)$  intensity ratio (Fig. 1) and in peak widths (Fig. 2 (b)) for *trans*-(CH)<sub>x</sub>  $\omega_1$  and  $\omega_3$  peaks that become transformed when the  $\hbar\omega_L$  exceeds the band gap ( $\sim 1.5 \text{ eV}$ <sup>4,13</sup>) indicative of resonant probing of an inhomogeneous chain. Our results show

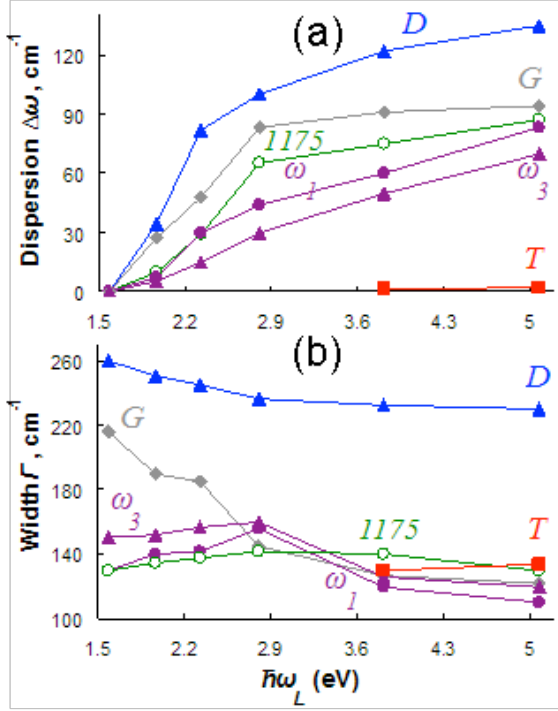


FIG. 2. (a) Peak dispersion,  $\Delta\omega$  and (b) peak widths,  $\Gamma$  for all constituent peaks as a function of the laser excitation energy  $\hbar\omega_L$ .

that inhomogeneity of intercalated  $trans$ -(CH) $_x$  chains measured using the distribution of the  $e$ -ph coupling constant  $\lambda$ ,  $p(\lambda)$  of the amplitude mode (AM) theory proposed by Ehrenfreund *et al.*<sup>3</sup> gives  $\lambda \sim 0.17$  for N-IR and  $\sim 0.24$  for UV; in good agreement with the AM model.  $\lambda$  determines the Peierls relation for the energy gap and its distribution arises from finite localisation lengths and bond length disorder. The AM results indicate that  $trans$ -(CH) $_x$  chains probed by high  $\hbar\omega_L$  are of shorter  $\pi$ -conjugation lengths and of higher bond disorder. The approximate chain lengths for both single  $C$ - $C$  and double  $C=C$  bonds of  $trans$ -(CH) $_x$  segments were determined using the bimodal distribution model proposed by Brivio *et al.*<sup>13</sup> and was found to be  $\sim 120$  of bond lengths units (N-IR), at the estimation limit of the model, and with a population

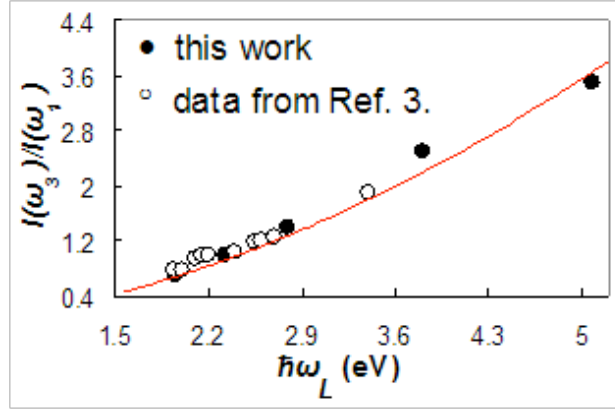


FIG. 3. The intensity ratio of  $I(\omega_3)/I(\omega_1)$  vs. the laser excitation energy  $\hbar\omega_L$  for *trans*-(CH)<sub>x</sub> inclusions in *a*-C:H. Solid line is a theoretical calculation performed using the amplitude mode formalism<sup>3</sup>.

of short chain of approximately 8 (UV). Shorter chains are probed by higher  $\hbar\omega_L$ . The average chain population is  $\sim 25 (\pm 5)$  bond length units owing to the uncertainties given by the Raman fitting and the bi-modal distribution model<sup>13</sup>. All *trans*-(CH)<sub>x</sub> chains are highly disordered as evidenced by wide  $\omega_1$  and  $\omega_3$  Raman peaks reaching their maximum in the blue-green range.

We have extended the  $I(\omega_3)/I(\omega_1)$  vs.  $\hbar\omega_L$  theoretical AM distribution calculations (independent of chain length) of Ehrenfreund *et al.*<sup>3</sup> for the visible range to include N-IR and UV  $\hbar\omega_L$ . Fig. 3 shows that our experimental results are in good agreement with the theoretical prediction and with Ehrenfreund's experimental data; clearly both the free-standing and incorporated *trans*-(CH)<sub>x</sub> chains obey the same  $I(\omega_3)/I(\omega_1)$  evolution formalism.

Long *trans*-(CH)<sub>x</sub> chains and PPV inclusions are only possible in an ordered  $sp^2$  *a*-C:H matrix that is achieved via deposition in ICP reactor analogous to used by Chen

*et al.*<sup>10</sup> with high plasma density and low electron temperature compared to conventional DLC deposition systems.

In summary, the RRS investigation of ICP fabricated *a*-C:H films showed that films host long *trans*-(CH)<sub>x</sub> chains with up to 120 C=C bond length units and also poly(*p*-phenylene vinylene) as evidenced by the 1175 cm<sup>-1</sup> Raman mode. We have postulated the origin of this PPV mode and provided a theoretical basis for arguing the response of *trans*-(CH)<sub>x</sub> chains in the *a*-C:H matrix to changing Raman excitation energy is identical to of free-standing chains. The evolution of relative intensity ratio for core *trans*-(CH)<sub>x</sub> modes will facilitate identification of *trans*-(CH)<sub>x</sub> modes in other complex carbonaceous materials spectra.

#### ACKNOLEGEMENTS

This work was supported by the Australian Research Council (LP0235814) and BAM research fellowship funding.

## REFERENCES

- <sup>1</sup> T. López-Ríos, É. Sandré, S. Leclercq, and É. Sauvain, *Phys. Rev. Lett.* **76**, 4935 LP (1996).
- <sup>2</sup> F. Piazza, A. Golanski, S. Schulze, and G. Relihan, *Appl. Phys. Lett.* **82**, 358 (2003).
- <sup>3</sup> E. Ehrenfreund, Z. Vardeny, O. Brafman, and B. Horovitz, *Phys. Rev. B* **36**, 1535 LP (1987).
- <sup>4</sup> A. J. Heeger, S. Kivelson, J. R. Schrieffer, and W.-P. Su, *Rev. Modern Phys.* **60**, 781 LP (1988).
- <sup>5</sup> A. J. Heeger, *Rev. Modern Phys.* **73**, 681 (2001).
- <sup>6</sup> A. Ferrari and J. Robertson, *Phys. Rev. B* **63**, 121405 (2001).
- <sup>7</sup> A. Hu, M. Rybachuk, Q. B. Lu, and W. W. Duley, *Appl. Phys. Lett.* **91**, 131906 (2007).
- <sup>8</sup> A. Hu, Q.-B. Lu, W. W. Duley, and M. Rybachuk, *J. Chem. Phys.* **126**, 154705 (2007).
- <sup>9</sup> G. A. J. Amaratunga, M. Chhowalla, C. J. Kiely, I. Alexandrou, R. Aharonov, and R. M. Devenish, *Nature* **383**, 321 (1996).
- <sup>10</sup> L.-Y. Chen and F. C.-N. Hong, *Appl. Phys. Lett.* **82**, 3526 (2003).
- <sup>11</sup> I. K. Varga, *J. Vacuum Sci. Tech. A* **7**, 2639 (1989).
- <sup>12</sup> A. C. Ferrari and J. Robertson, *Phys. Rev. B* **64**, 075414 (2001).
- <sup>13</sup> G. P. Brivio and E. Mulazzi, *Phys. Rev. B* **30**, 876 (1984).
- <sup>14</sup> M. Rybachuk and J. M. Bell, *Diamond Rel. Mat.* **15**, 977 (2006).
- <sup>15</sup> D. C. Benner, C. P. Rinsland, V. M. Devi, M. A. H. Smith, and D. Atkins, *J. Quant. Spec. Radiat. Transfer* **53**, 705 (1995).

- <sup>16</sup> D. B. Fitchen, *Molecul. Cryst. Liq. Cryst.* **83**, 95 (1982).
- <sup>17</sup> V. Hernandez, C. Castiglioni, M. Del Zoppo, and G. Zerbi, *Phys. Rev. B* **50**, 9815 (1994).
- <sup>18</sup> M. Tzolov, V. P. Koch, W. Bruetting, and M. Schwoerer, *Synth. Metals* **109**, 85 (2000).
- <sup>19</sup> I. Orion, J.-P. Buisson, and S. Lefrant, *Phys. Rev. B* **57**, 7050 (1990).
- <sup>20</sup> M. Baitoul, J. Wery, J.-P. Buisson, G. Arbuckle, H. Shah, S. Lefrant, and M. Hamdome, *Polymer* **41**, 6955 (2000).